Quaternary Science Reviews 158 (2017) 164–171

Contents lists available at ScienceDirect

Quaternary Science Reviews

journal homepage: www.elsevier.com/locate/quascirev

Multi-proxy dating the 'Millennium Eruption' of Changbaishan to late 946 CE

Clive Oppenheimer [a,*], Lukas Wacker [b], Jiandong Xu [c], Juan Diego Galván [d], Markus Stoffel [e,f,g], Sébastien Guillet [g], Christophe Corona [h], Michael Sigl [i], Nicola Di Cosmo [j], Irka Hajdas [b], Bo Pan [c], Remco Breuker [k], Lea Schneider [l], Jan Esper [l], Jie Fei [m], James O.S. Hammond [n], Ulf Büntgen [a,d]

[a] Department of Geography, University of Cambridge, Cambridge, United Kingdom
[b] Laboratory of Ion Beam Physics, ETH Zurich, Zurich, Switzerland
[c] Key Laboratory of Active Tectonics and Volcano, Institute of Geology, China Earthquake Administration (CEA), Beijing, China
[d] Swiss Federal Research Institute WSL, Birmensdorf, Switzerland
[e] Institute for Environmental Sciences, University of Geneva, Geneva, Switzerland
[f] Department of Earth Sciences, University of Geneva, Geneva, Switzerland
[g] Dendrolab.ch, Institute of Geological Sciences, University of Bern, Bern, Switzerland
[h] Geolab UMR6042 CNRS, Université Blaise Pascal, Clermont-Ferrand, France
[i] Paul Scherrer Institut, Villigen, Switzerland
[j] School of Historical Studies, Institute for Advanced Study, Princeton, NJ, USA
[k] Leiden Institute for Area Studies, University of Leiden, Leiden, The Netherlands
[l] Department of Geography, Johannes Gutenberg University, Mainz, Germany
[m] Institute of Chinese Historical Geography, Fudan University, Shanghai, China
[n] Department of Earth and Planetary Sciences, Birkbeck College, University of London, London, United Kingdom

ARTICLE INFO

Article history:
Received 3 November 2016
Received in revised form
9 December 2016
Accepted 10 December 2016

Keywords:
Holocene
Paleoclimatology
Eastern Asia
Cosmogenic isotopes
Ice cores
Tree-rings

ABSTRACT

Ranking among the largest volcanic eruptions of the Common Era (CE), the 'Millennium Eruption' of Changbaishan produced a widely-dispersed tephra layer (known as the B-Tm ash), which represents an important tie point for palaeoenvironmental studies in East Asia. Hitherto, there has been no consensus on its age, with estimates spanning at least the tenth century CE. Here, we identify the cosmogenic radiocarbon signal of 775 CE in a subfossil larch engulfed and killed by pyroclastic currents emplaced during the initial rhyolitic phase of the explosive eruption. Combined with glaciochemical evidence from Greenland, this enables us to date the eruption to late 946 CE. This secure date rules out the possibility that the Millennium Eruption contributed to the collapse of the Bohai Kingdom (Manchuria/Korea) in 926 CE, as has previously been hypothesised. Further, despite the magnitude of the eruption, we do not see a consequent cooling signal in tree-ring-based reconstructions of Northern Hemisphere summer temperatures. A tightly-constrained date for the Millennium Eruption improves the prospect for further investigations of historical sources that may shed light on the eruption's impacts, and enhances the value of the B-Tm ash as a chronostratigraphic marker.

1. Introduction

The 'Millennium Eruption' of Changbaishan volcano (also known as Mt. Paektu and Baegdusan), is so-called because it has been thought to have occurred approximately 1000 CE. The volcano is located on the border between China and the Democratic People's Republic of Korea (Fig. 1a and b). The Millennium Eruption disgorged an estimated 24 km^3 of dense magma (Horn and Schmincke, 2000), mostly as rhyolitic (comendite) tephra but with a subordinate quantity of trachyte. Stratigraphic relationships demonstrate clearly that the rhyolitic magma was erupted before the trachytic magma. Based on pumice clast size distributions, Horn and Schmincke estimated that the eruption column easily passed the tropopause. The tephra fallout associated with the rhyolitic

* Corresponding author.
E-mail address: co200@cam.ac.uk (C. Oppenheimer).

http://dx.doi.org/10.1016/j.quascirev.2016.12.024

stage of the eruption extends across northeast China (Sun et al., 2015), the far-east costal region of Russia (Andreeva et al., 2011) and the Korean peninsula. It is found in deep-sea sediment cores from the Japan Sea (Machida and Arai, 1983), as well as in lacustrine and peat sedimentary archives from Japan (e.g., Hughes et al., 2013; Chen et al., 2016; McLean et al., 2016, Fig. 1c). Known as the Baegdusan-Tomakomai ash (B-Tm layer), it represents a key stratigraphic marker in palaeoenvironmental and archaeological contexts (Chen et al., 2016). Millennium Eruption tephra have also been identified in a high-resolution ice core (NEEM-2011-S1) from northern Greenland (Sun et al., 2014a). Despite substantial efforts to date the paroxysm, mostly using radiocarbon techniques, the resulting estimates span at least the tenth century CE (Fig. 2; Sun et al., 2014b). Attempts to date the eruption have also prompted searches of mediaeval texts for reports suggestive of volcanic phenomena (Hayakawa and Koyama, 1998).

Among more recent attempts to date the Millennium Eruption are two works based on wiggle-matched radiocarbon ages of trees (*Pinus* and *Larix*) that were engulfed (alive) by pyroclastic density currents during the eruption (Xu et al., 2013; Yin et al., 2012), and another based on Greenland ice core stratigraphy (Sun et al., 2014a). These studies pointed to an eruption date sometime in the period between the 920s and 950s CE.

We set out here to calculate an accurate date of the Millennium Eruption by making new radiocarbon measurements of the same subfossil larch stem from China, for which previous wiggle-matching (Xu et al., 2013) yielded a model age of 940–952 CE (2σ) for the outermost ring before bark (*waldkante*). Since the tree was 264 years old when killed by the eruption, we reasoned that it was alive in 775 CE, the year of an ephemeral burst of cosmogenic radiation. The signature of this event has been recognized in annually-resolved ^{14}C measurements made for trees from Japan (Miyake et al., 2012), Europe (Büntgen et al., 2014), and New Zealand (Güttler et al., 2015), as well as in ^{10}Be abundance in ice cores from Greenland and Antarctica (Sigl et al., 2015). We hypothesized that locating this absolute time marker would enable simple annual increment counting to date the last ring formed by our tree before it was killed by the Millennium Eruption. A secure date for the Millennium Eruption would permit us to investigate the magnitude and extent of any climate response using Northern Hemisphere summer temperature proxies.

2. Materials and methods

The studied subfossil trunk (Fig. 3) belongs to a mature *Larix*, which would have had an estimated crown height of 20 m. The deposits containing the tree are located at Xiaoshahe on the northwest flank of Changbaishan volcano, about 24 km from the summit caldera (Fig. 1a). These deposits are of rhyolitic composition belonging to the first phase of the Millennium Eruption – the glass

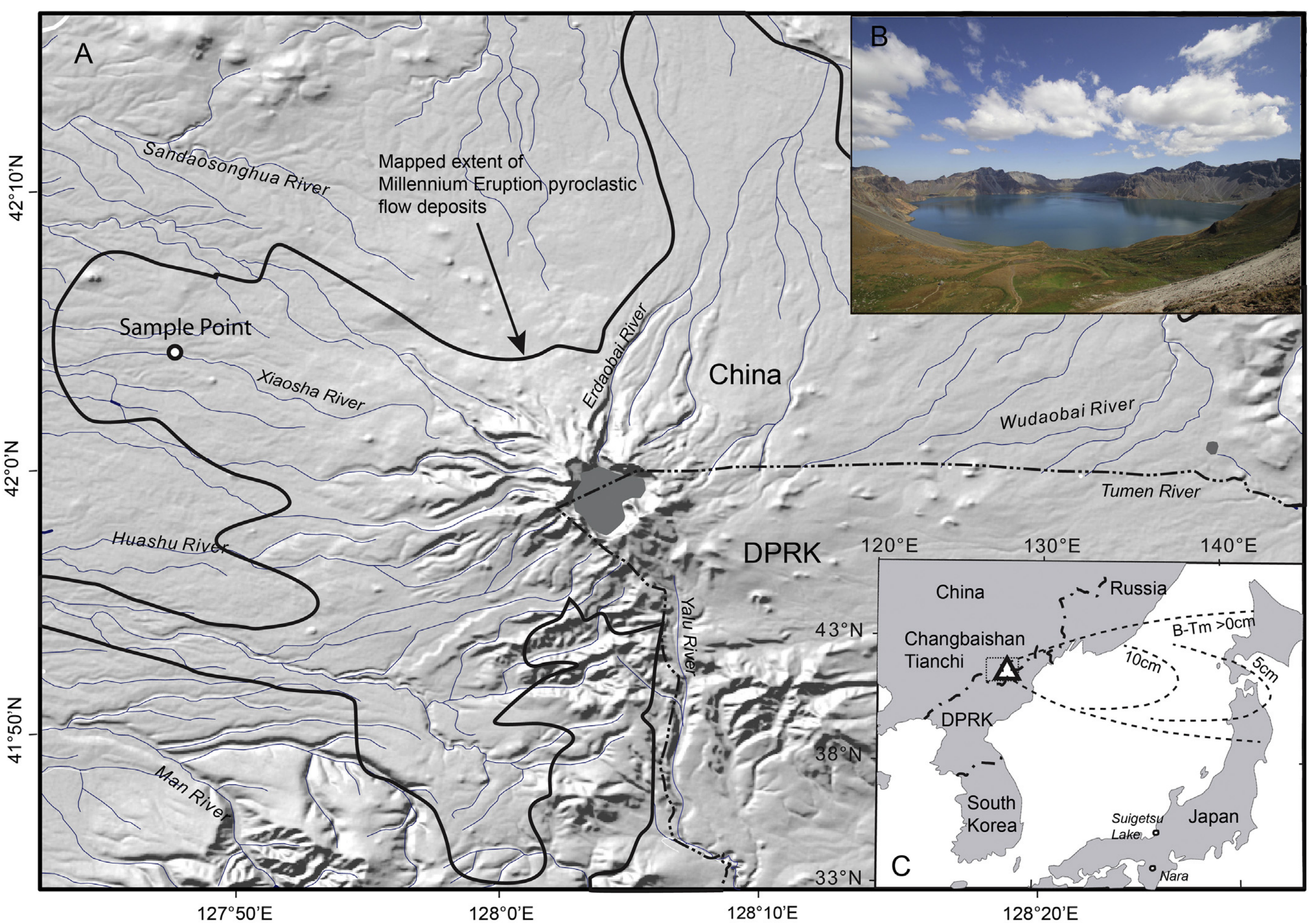

Fig. 1. Contextual information for the Millennium Eruption. (A) Location of the volcano and the tree sampling site (labelled 'Sample Point', 42°05.67′N; 127°47.87′E). (B) Photograph of the summit caldera and lake, taken from the Chinese side of the volcano. (C) Isopach map for the B-Tm layer (after Machida and Arai, 1983), showing sites in Japan discussed in the text.

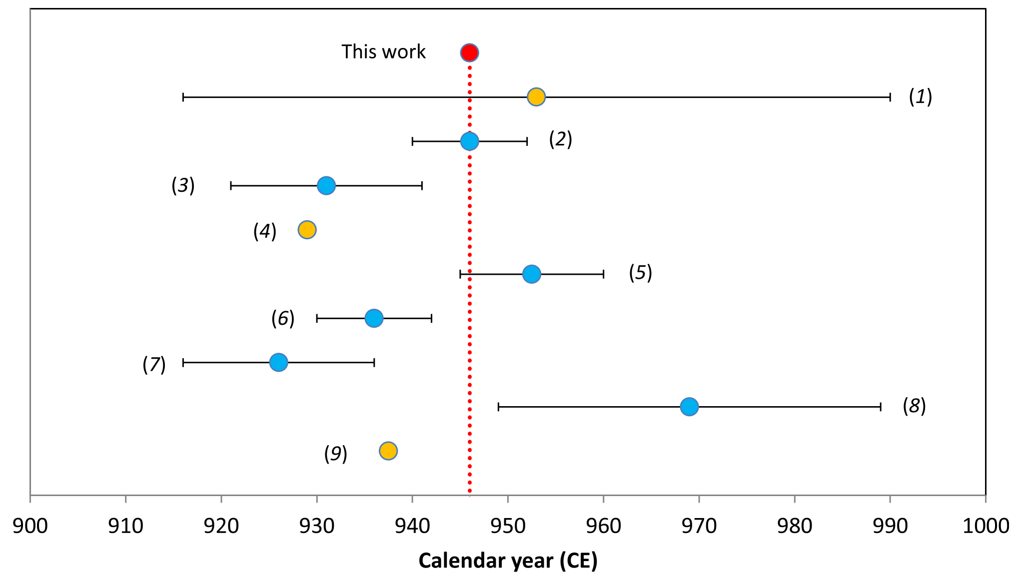

Fig. 2. Selected radiocarbon (blue symbols) and varve-based (yellow symbols) age estimates for the Millennium Eruption (1: Sun et al., 2015; 2: Xu et al., 2013; 3: Yin et al., 2012; 4: Kamite et al., 2010; 5: Yatsuzuka et al., 2010; 6: Nakamura et al., 2007; 7: Machida and Okumura, 2007; 8: Horn and Schmincke, 2000; 9: Fukusawa et al., 1998). The red-dotted line indicates the year 946 CE calculated in our analysis. Two-sigma uncertainties on model ages are shown by whiskers. (For interpretation of the references to colour in this figure legend, the reader is referred to the web version of this article.)

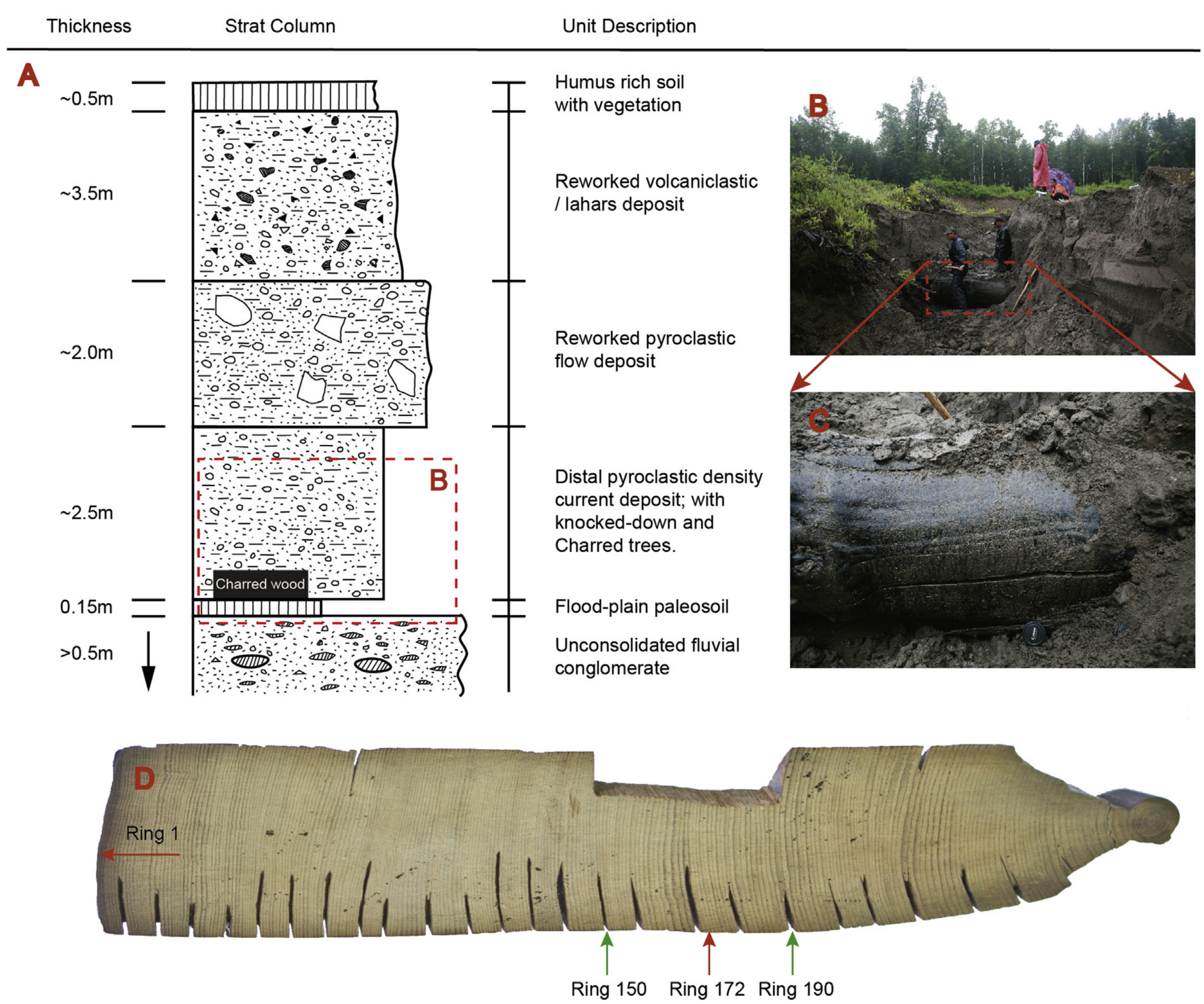

Fig. 3. Context for the sampled *Larix* stem. (A) Stratigraphic section showing location of tree. (B) The tree *in situ* at the sampling location; the deposits encasing it correspond to the part of the stratigraphy highlighted by the dashed box labelled ‘B’ in the schematic section to the left. (C) a close-up view of the tree. (D) Cross-section of sampled trunk (approximately 0.35 m radius) showing selected ring numbers.

chemistry matches very closely that reported for both proximal and distal samples (Table 1). The tree stem, of which a 3 m length was recovered, has a diameter of 0.73 m, and is severed from the roots. It was found aligned in the direction of flow of the pyroclastic density currents, as indicated by sedimentary structures in the pumiceous deposits, and consistent with the local slope. The bark is partially charred, pointing to the high temperature of the pyroclastic currents that engulfed the tree. This combination of observations strongly suggests that the tree was killed as a result of being exposed to the pyroclastic currents associated with the initial rhyolitic stage of the Millennium Eruption.

Rings were counted inwards from the *waldkante*. Growth is fairly complacent, and average ring width is approximately 2 mm. Based on previously published radiocarbon-ages and a reported ^{14}C outlier (Xu et al., 2013), we made new sequential ^{14}C analyses of rings between tree age 168 and 177, hoping to identify the 775 CE cosmogenic signal and thereby date (to the year) the preserved annual growth increments of the subfossil larch.

Holocellulose was isolated from each individual growth ring (Nemec et al., 2010), and converted to graphite for high-precision radiocarbon measurements on the compact MICADAS radiocarbon facility at ETH Zurich (Synal et al., 2007). Samples were washed at near neutral pH between each step. Graphitization was carried out using the 'AGE' system (Wacker et al., 2010a), employing pre-cleaned iron as a catalyst. The subsequent ^{14}C measurements were made with a MICADAS tandem accelerator (Wacker et al., 2010b). We compared our data with a high-temporal resolution calibration curve based on published dendrochronologically-dated, annually-resolved tree-ring measurements from Japan and Europe around the 775 CE event.

We also investigated high-resolution ice-core data for the NEEM-2011-S1 ice core from northern Greenland (located at 77.45°N and 51.06°W; Jensen et al., 2014). This is the same core in which Millennium Eruption tephra (both rhyolitic and trachytic compositions) were identified (Sun et al., 2014a). To supplement available data for non-sea-salt sulphur (nssS), non-sea-salt calcium (nssCa) and chlorine (Cl) concentrations, determined by inductively coupled plasma mass spectrometry and using continuous flow analysis (Sigl et al., 2013), we carried out a replicate analysis on a parallel ice-core section. The original data coverage between 247.20 and 248.90 m depth (circa 939–947 CE) was 91% for (Sigl et al., 2013; Sun et al., 2014a) but we achieved 96% with our replicate analysis, enabling better identification of annual layers. The largest remaining data gap is 10 cm (corresponding to <6 months), and three years before the Millennium Eruption signature. This was associated with an internal fracture that was removed prior to continuous flow analysis just in case it had been contaminated with core drilling fluid. Annual layer thickness from circa 939 to 947 CE is 0.205 ± 0.026 m per year compared with 0.205 ± 0.025 m per year for the interval circa 900–999 CE. The seasonal and annual cycles are best resolved in nssCa (winter/spring maximum) and Cl concentrations (winter maximum).

Lastly, we generated reconstructions of Northern Hemisphere (NH) summer temperature anomalies (NH1, NH2) using a recent compilation of 14 tree-ring width (TRW) and 16 maximum latewood density (MXD) site chronologies spanning the past 1500 years (Stoffel et al., 2015; Guillet et al., in press). MXD time-series exhibit less biological memory at interannual scale when compared with TRW data (Frank et al., 2007), and are therefore better suited to identification of the abrupt and relatively ephemeral effects of volcanic eruptions on NH summertime temperatures (Esper et al., 2015; Schneider et al., 2015).

NH1 is based on a linear model using principal component analysis to calibrate 30 regional tree-ring (TRW and MXD) clusters against a mean of instrumental June-July-August (JJA) 40–90°N land only temperatures (1805–1976) (BEST; http://berkeleyearth.org/data/). The calibration and validation process was repeated 1000 times using a bootstrap method so as to assess the robustness of the reconstruction. To account for the decreased number of chronologies back in time, a nested approach was used to maximize reconstruction length and to evaluate uncertainties. The final reconstruction was developed by splicing all of the nested time series ($n = 32$). The mean and variance of each nested reconstruction had been adjusted to the best replicated nest (1775–1976). Calibration and validation statistics ($R^2 = 0.25$–0.51, $r^2 = 0.19$–0.45, Reduction of Error (RE) = 0.20–0.47, coefficient of efficiency (ce) = 0.18–0.45) confirm the reliability of the reconstruction (Stoffel et al., 2015).

NH2 accounts for the spatial variability of volcanic cooling and is based on a two-step procedure. First, linear regression analysis was used in each cluster to calibrate the cluster series to JJA gridded-temperature anomalies (with respect to 1961–1990) from the Climatic Research Unit (CRU) and BEST data sets. For each cluster, we kept either the CRU or BEST reconstruction, depending on the significance level of the verification (RE, ce) statistics. Seven reconstructions failing classical calibration and verification tests were excluded from the final NH2 reconstruction. Averaging was performed to composite 23 cluster reconstructions into the NH2 chronology.

3. Results and discussion

Table 2 reports the results of the radiocarbon analysis. From a significant step-function in the radiocarbon age sequence, we

Table 1
Glass composition for samples of distal pyroclastic density current deposits that entomb the subfossil larch at Xiaoshahe, compared with other samples of Millennium Eruption rhyolite (comendite).

	Xiaoshahe (this study)[a]	Proximal rhyolite[b]	B-Tm (type material)[c]	Lake Suigetsu, Japan[c]	Greenland (QUB-1819b)[d]
SiO_2	73.4 ± 0.99	74.8 ± 0.27	73.7 ± 2.4	74.6 ± 1.8	74.7 ± 0.45
TiO_2	0.24 ± 0.02	0.20 ± 0.04	0.24 ± 0.07	0.23 ± 0.07	0.22 ± 0.03
Al_2O_3	11.3 ± 0.6	10.6 ± 0.18	11.2 ± 1.5	10.5 ± 1.1	10.6 ± 0.5
FeO	4.29 ± 0.11	4.05 ± 0.09	4.09 ± 0.21	4.07 ± 0.17	4.1 ± 0.25
MnO	0.09 ± 0.01	0.08 ± 0.05	–	–	0.045 ± 0.020
MgO	0.021 ± 0.009	0.02 ± 0.02	–	–	0.024 ± 0.011
CaO	0.33 ± 0.11	0.26 ± 0.04	0.37 ± 0.26	0.26 ± 0.23	0.29 ± 0.09
Na_2O	5.29 ± 0.34	5.32 ± 0.34	5.34 ± 0.32	5.36 ± 0.15	5.0 ± 0.5
K_2O	4.66 ± 0.14	4.52 ± 0.10	4.49 ± 0.31	4.43 ± 0.34	4.53 ± 0.26
Cl	0.41 ± 0.04	–	0.47 ± 0.11	0.48 ± 0.08	0.46 ± 0.02
n	13	10	21	30	4

[a] Measurements made by electron microprobe analysis.
[b] Original sources listed in Sun et al. (2014b).
[c] Type B-Tm material from Port Tomakomai, Hokkaido (McLean et al., 2016).
[d] Shards from the NEEM-2011-S1 ice core, Greenland (Sun et al., 2014a).

Table 2
Radiocarbon measurements for the subfossil larch.

Ring #	Lab reference	$F^{14}C$	Radiocarbon age (yr)	$\delta^{13}C$ (‰)
168	ETH-60227	0.8640 ± 0.0019	1174 ± 18	−21.2
169	ETH-60228	0.8665 ± 0.0020	1151 ± 18	−21.3
170	ETH-60229	0.8675 ± 0.0020	1142 ± 18	−19.3
171	ETH-60230	0.8640 ± 0.0014	1175 ± 13	−20.8
172	ETH-60231	0.8653 ± 0.0021	1162 ± 19	−20.2
173	ETH-60232	0.8538 ± 0.0014	1270 ± 13	−21.7
174	ETH-60233	0.8512 ± 0.0020	1294 ± 19	−20.0
175	ETH-60234	0.8491 ± 0.0020	1314 ± 19	−20.8
176	ETH-60235	0.8508 ± 0.0020	1298 ± 19	−18.2
177	ETH-60236	0.8484 ± 0.0019	1321 ± 18	−20.4

determined that ring 172 was formed in 775 CE (Fig. 4; ring identified in Fig. 3). This dates the *waldkante* to 946 CE. The presence of latewood in the *waldkante* indicates that the eruption occurred either towards the very end of the growing season in autumn that year or during the subsequent winter dormancy. Shifting the calibration curve by one year to date the *waldkante* to 947 CE offers the next-best fit from a statistical perspective but increases the χ^2 substantially from 10.6 to 38.3, indicating a highly unlikely fit (95% limit: $\chi^2 = 19.1$). Our date reveals that the estimation by Xu et al. (2013) was the most accurate of the many prior attempts to date the Millennium Eruption.

Examination of the sub-annual resolution chlorine (Cl), non-sea salt calcium (nssCa) and non-sea salt sulphur (nssS) stratigraphy for the Greenland ice core, NEEM-2011-S1, which contains Millennium Eruption tephra (Sun et al., 2014a), enables us to constrain further the timing of the eruption. Seasonality is pronounced for nssCa (typically peaking in late winter/spring; Kang et al., 2015) and Cl (peaking in midwinter; Davidson et al., 1989). Focusing on the core section containing Millennium Eruption tephra, we observe near synchronous peaks in nssS, nssCa and Cl (Fig. 5). Assuming the Millennium Eruption plume was transported close to the tropopause (Herzog and Graf, 2010), and accounting for the typical action of cold-season planetary waves (Perlwitz and Graf, 1995), a typical time interval between eruption and sulphate aerosol deposition over northern Greenland is 1–2 months. This narrows the Millennium Eruption time window to the last 2 or 3 months of 946 CE. A later eruption, in mid- or late winter, is unlikely, since a strengthened polar vortex would have delayed volcanic aerosol deposition over the Arctic until spring, such that the nssS peak would have lagged behind the Cl peak.

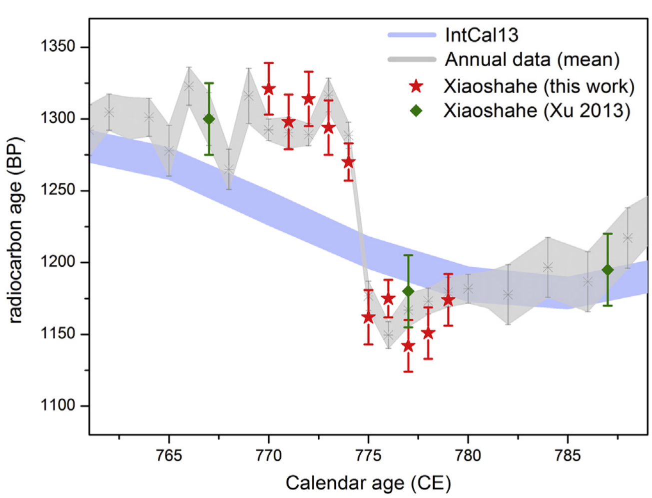

Fig. 4. High-resolution radiocarbon ages (red and green) superimposed on annually-resolved radiocarbon measurements from Japan (Miyake et al., 2012) and Europe (Büntgen et al., 2014; Wacker et al., 2014) (grey trace and dots). The IntCal13 ^{14}C calibration curve (Reimer et al., 2013) is also shown (blue). Ring 172 corresponds to 775 CE. Uncertainties are 1-σ estimates. (For interpretation of the references to colour in this figure legend, the reader is referred to the web version of this article.)

Our dating of the Millennium Eruption, corroborates the finding of Sigl et al. (2015) that the Greenland Ice Core Chronology 2005 (GICC05) timescale is six years adrift in this period. Such a discrepancy had already been suggested based on the timing of volcanic markers in tree rings and ice cores (Baillie, 2008). The shift is not only of significance when assessing the climate forcing (determined from tree-ring chronologies) of volcanic eruptions (identified in ice core records; e.g., Anchukaitis et al., 2012), but also when examining associations between volcanic forcing, climate change and historical events (e.g., Oppenheimer, 2011, 2015; Büntgen et al., 2014, 2016).

We next assess the climate response of the Millennium Eruption using the two tree ring-based reconstructions (Fig. 6). We find no significant cooling in 947 CE that could be attributed to the effects of the Millennium Eruption, neither in NH1 (−0.44 °C, rank 133) nor in NH2 (−0.31, rank 253). This muted temperature response appears consistent with the modest sulphur abundance collocated with the Millennium Eruption tephra layer in the NEEM-2011-S1 ice core (Fig. 5), consistent with other Greenland ice cores (Zielinski, 1995; Sigl et al., 2015) and the sulphur yield estimated by Horn and Schmincke (2000) from petrological data. Based on volatile abundances in crystal-hosted melt inclusions in Millennium Eruption tephra, Iacovino et al. (2016) argued that the eruption could have released up to 45 Tg of sulphur to the atmosphere. Such a high yield (five times the sulphur released by the 1991 eruption of Mount Pinatubo) appears at odds with the testimony of ice cores and tree rings. We note that the figure calculated by Iacovino et al. (2016) represents an upper estimate of the sulphur output. If the true sulphur yield approached such a high value, then the discrepancy with the ice core and tree ring records is curious.

3.1. Historical sources

Mediaeval chronicles inform us that Changbaishan was a sacred place of cult for Manchurian peoples. Following the downfall of the Tang dynasty in 907 CE, the area was part of the Bohai kingdom until its defeat in 926 CE (Kim, 2011). Several scholars have linked the collapse of the Bohai state to the Millennium Eruption (Machida et al., 1990; Kim, 2011). However, our finding demonstrates that the Millennium Eruption post-dates the fall of the Bohai kingdom by twenty years, and we can reject this hypothesis. Of the medieval texts suggestive of phenomena associated with the Millennium Eruption, the most concordant with our new dating is an observation in 946 CE recorded in the *Koryŏsa* (history of the Koryŏ dynasty), which reads 是岁, 天鼓鸣, 赦. This attests to the manifestation, at the palace in Kaesŏng, of a loud disturbance: “That year the sky rumbled and cried out, there was an amnesty”. The implication is that this loud noise coming from the sky may have been taken as an omen that prompted the pardoning of convicts. Kaesŏng is approximately 470 km from Changbaishan, a distance that is well within the range over which the detonations of comparably large explosive eruptions have been heard in the past, for instance during the 1815 eruption of Tambora (Oppenheimer, 2003). This distance could also place Kaesŏng beneath the umbrella cloud likely to have been associated with the Millennium Eruption.

Also of note, the Heungboksa Temple History from Nara (Japan) records that “white ash fell gently like snow” on 3 November 946 CE (Hayakawa and Koyama, 1998). Although Nara lies approximately 1000 km southeast from Changbaishan, and some 700 km from the dispersal axis of the B-Tm layer as shown in Fig. 1c, clear evidence that Millennium Eruption ash fell in this region is

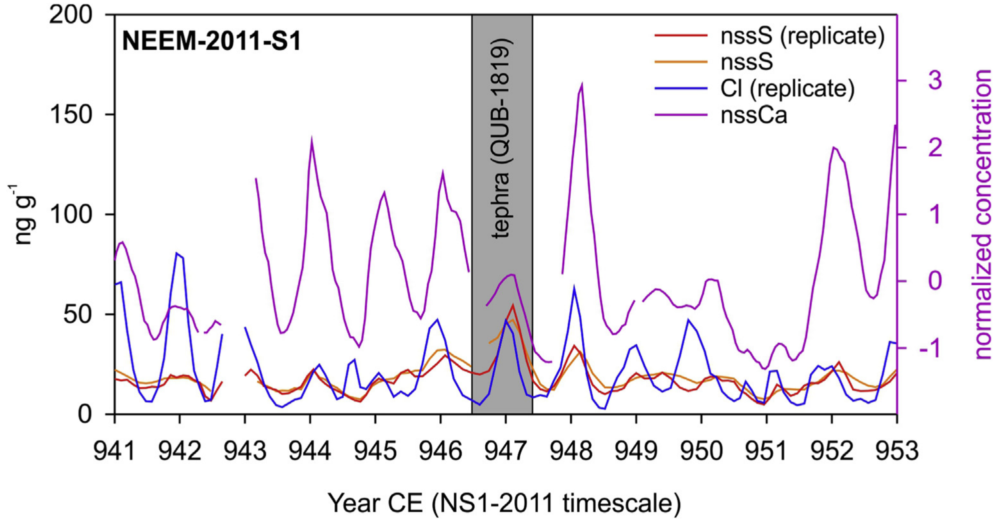

Fig. 5. NEEM-2011-S1 glaciochemistry. Chloride, non-seasalt calcium (nssCa) and non-seasalt sulphur (nssS) concentrations are shown (corrected for marine sources of sulphur and MSA). The grey box indicates the section of core in which tephra, matching both the rhyolitic and trachytic compositions of the Millennium Eruption, were extracted (Sun et al., 2014a). The timescale is equivalent to (GICC05 + 6 years). Note the relatively weak nssS signal associated with the Millennium Eruption. (For a colour version of this figure, the reader is referred to the web version of this article.)

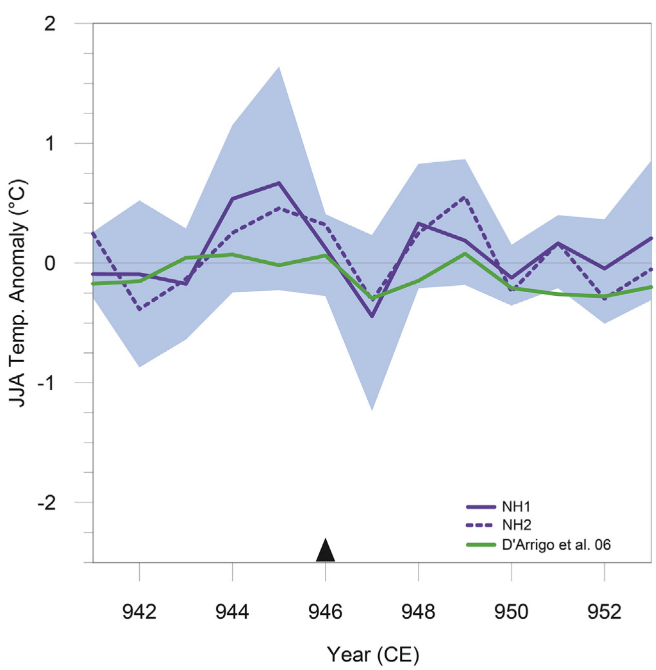

Fig. 6. Tree ring-based land-only Northern Hemisphere (40–90°N) summer (JJA) temperature anomalies (NH1 and NH2; Stoffel et al., 2015). The blue shaded area denotes the uncertainties (2.5 and 97.5 percentile) related to the NH1 tree-ring reconstruction, which were estimated using a bootstrap method applied to the calibration/validation. The Millennium Eruption is not associated with a statistically-significant summer cooling in this proxy record. Green line shows tree-ring-width-only reconstruction for comparison (D'Arrigo et al., 2006). (For interpretation of the references to colour in this figure legend, the reader is referred to the web version of this article.)

provided by its presence in the sediment sequence from Lake Suigetsu, which is just 100 km north from Nara (McLean et al., 2016). Significantly, the composition of this ash is rhyolitic, and its glass composition matches closely that of the tephra that engulfed our tree sample (as well as that of proximal samples of Millennium Eruption deposits and of the shards extracted from the NEEM-2001-S1 ice core; Table 1). These correspondences point to a common, widely-dispersed deposit associated with the paroxysmal, ignimbrite-forming eruption. Considering the scale of umbrella clouds associated with large explosive eruptions, it is unsurprising that tephra could have dispersed over such a wide region. For comparison, the umbrella cloud for the smaller eruption of Pinatubo in 1991 reached more than 1000 km across (Holasek et al., 1996). While Japan has many active volcanoes, Nara lies several hundred kilometres from the nearest local sources. This report of ash fallout is, therefore, likely to represent a rare event. Ash sourced from Changbaishan could reach Japan within a day, transported by typical lower stratospheric airflow.

4. Conclusions and final remarks

We date the Millennium Eruption of Changbaishan volcano (also known as Mount Paektu and Tianchi volcano) to late 946 CE using the 775 CE cosmogenic event as an exact time marker in a tree killed by the eruption, combined with inspection of high-resolution glaciochemical data for the NEEM ice core (Greenland). Observations recorded in two historical sources could be interpreted as signs of the eruption (sounds of the explosions and ashfall). Testimony of ash fallout in Nara, Japan, on 3 November 946, might pinpoint the Millennium Eruption's main phase within a day. But we should be cautious in regarding these reports as certain manifestations of the eruption – they are too ambiguous for that.

State-of-the-art tree ring-based Northern Hemisphere summer temperatures reconstructions reveal, at most, a muted response to the Millennium Eruption, notwithstanding the magnitude of the event. The apparently weak cooling effect and the limited sulphur attributable to the Millennium Eruption recorded in the NEEM-2011-S1 ice core from Greenland appear to contradict petrological arguments for a very substantial sulphur release to the atmosphere (Iacovino et al., 2016). Further investigation will be required to reconcile these findings.

Our work demonstrates the remarkable potential of utilising abrupt cosmogenic signatures found in tree-rings for the precise dating of volcanic events. By securing the age of the widespread B-Tm layer, its use for stratigraphic purposes is enhanced and high-resolution timescales can be recalibrated (Nanayama et al., 2003). Previously, ages of 937–8 and 929 CE have been estimated for the

Millennium Eruption by counting lacustrine varves between the B-Tm and an older tephra sourced from Towada volcano (To-a) found in lake sediments in Japan (Kamite et al., 2010; Yamada et al., 2010). These estimates have assumed that the To-a ash dates to 915 CE. However, the discrepancy between the varve-based estimates and our calendrical date for the ME is sufficiently large to call into question the accepted date of the To-a tephra, which may instead have been erupted in the 920s or 930s CE.

Acknowledgments

CO acknowledges the support of the Lounsbery Foundation for research on Changbaishan/Paektu volcano, and from the NERC Centre for the Observation and Modelling of Earthquakes, Volcanoes and Tectonics. Fieldwork support was provided by the ‘Special Projects’ of the Institute of Geology, China Earthquake Administration (IGCEA1505). DG was supported by the WSL-internal COSMIC project. UB was supported by the Ministry of Education, Youth and Sports of the Czech Republic under the National Sustainability Program I (NPU I), grant number LO1415. MS, SG, and CC received funding from the Era.Net RUS Plus project ‘Effects of Large Volcanic eruptions on Eurasian Climate and Societies: unravelling past evidence to predict future impacts’ (ELVECS; No. IZRPZ0_164735). We thank the anonymous reviewer for very beneficial comments on the original manuscript, and Professor José Carrión for editorial handling.

References

Anchukaitis, K.J., Breitenmoser, P., Briffa, K.R., Buchwald, A., Büntgen, U., Cook, E.R., D'Arrigo, R.D., Esper, J., Evans, M.N., Frank, D., Grudd, H., Gunnarson, B., Hughes, M.K., Kirdyanov, A.V., Körner, C., Krusic, P.J., Luckman, B., Melvin, T.M., Salzer, M.W., Shashkin, A.V., Timmreck, C., Vaganov, E.A., Wilson, R.J.S., 2012. No evidence for misdating of tree-ring chronologies associated with volcanic cooling. Nat. Geosci. 5, 836–837. http://dx.doi.org/10.1038/ngeo1645.

Andreeva, O.A., Naumov, V.B., Andreeva, I.A., Kovalenko, V.I., 2011. May. Basaltic melts in olivine from alkaline pumice of Primor'e: evidence from the study of melt inclusions. Dokl. Earth Sci. 438, 656–660.

Baillie, M.G.L., 2008. Proposed re-dating of the European ice core chronology by seven years prior to the 7th century AD. Geophys. Res. Lett. 35, L15813. http://dx.doi.org/10.1029/2008GL034755.

Büntgen, U., Myglan, V.S., Charpentier Ljungqvist, F., McCormick, M., Di Cosmo, N., Sigl, M., Jungclaus, J., Wagner, S., Krusic, P.J., Esper, J., Kaplan, J.O., de Vaan, M.A.C., Luterbacher, J., Wacker, L., Tegel, W., Kirdyanov, A.V., 2016. Cooling and societal change during the late Antique little ice age from 536 to around 660 AD. Nat. Geosci. 9, 231–236.

Büntgen, U., Wacker, L., Nicolussi, K., Sigl, M., Güttler, D., Tegel, W., Krusic, P.J., Esper, J., 2014. Extraterrestrial confirmation of tree-ring dating. Nat. Clim. Change 4, 404–405.

Chen, X.Y., Blockley, S.P., Tarasov, P.E., Xu, Y.G., McLean, D., Tomlinson, E.L., Albert, P.G., Liu, J.Q., Müller, S., Wagner, M., Menzies, M.A., 2016. Clarifying the distal to proximal tephrochronology of the Millennium (B–Tm) eruption, Changbaishan Volcano, northeast China. Quat. Geochronol. 33, 61–75.

D'Arrigo, R., Wilson, R., Jacoby, G., 2006. On the long-term context for late twentieth century warming. J. Geophys. Res. 111, D03103. http://dx.doi.org/10.1029/2005JD006352.

Davidson, C.I., et al., 1989. Seasonal variations in sulfate, nitrate and chloride in the Greenland ice sheet: relation to atmospheric concentrations. Atmos. Env. 23, 2483–2493.

Esper, J., Schneider, L., Smerdon, J., Schöne, B., Büntgen, U., 2015. Signals and memory in tree-ring width and density data. Dendrochronologia 35, 62–70.

Frank, D.C., Büntgen, U., Böhm, R., Maugeri, M., Esper, J., 2007. Warmer early instrumental measurements versus colder reconstructed temperatures: shooting at a moving target. Quat. Sci. Rev. 26, 3298–3310.

Fukusawa, H., Tsukamoto, S., Tsukamoto, H., Ikeda, M., Matsuoka, M., 1998. Falling age of Baegdusan-Tomakomai tephra (B-Tm) estimated by using non-glacial varves. Laguna 5, 55–62.

Guillet, S., Corona, C., Stoffel, M., Khodri, M., Lavigne, F., Ortega, P., Eckert, N., Selenniou, P., Daux, V., Churakova (Sidorova), O., Davi, N., Edouard, J.L., Yong, Z., Luckman, B.H., Myglan, V.S., Guiot, J., Beniston, M., Masson-Delmotte, V., Oppenheimer, C., 2017. Climate response to the 1257 Samalas eruption revealed by proxy records. Nat. Geosci. (in press).

Güttler, D., et al., 2015. Rapid increase in cosmogenic 14 C in AD 775 measured in New Zealand kauri trees indicates short-lived increase in ^{14}C production spanning both hemispheres. Earth Planet. Sci. Lett. 411, 290–297.

Hayakawa, Y., Koyama, M., 1998. Dates of two major eruptions from Towada and Baitoushan in the 10th century. Bull. Volcanol. Soc. Jpn. 43, 403–407.

Herzog, M., Graf, H.-F., 2010. Applying the three-dimensional model ATHAM to volcanic plumes: dynamic of large co-ignimbrite eruptions and associated injection heights for volcanic gases. Geophys. Res. Lett. 37, L19807. http://dx.doi.org/10.1029/2010GL044986.

Holasek, R.E., Self, S., Woods, A.W., 1996. Satellite observations and interpretation of the 1991 Mount Pinatubo eruption plumes. J. Geophys. Res. 101 (B12), 27635–27655. http://dx.doi.org/10.1029/96JB01179.

Horn, S., Schmincke, H.U., 2000. Volatile emission during the eruption of Baitoushan volcano (China/North Korea) ca. 969 AD. Bull. Volcanol. 61, 537–555.

Hughes, P.D.M., Mallon, G., Brown, A., Essex, H.J., Stanford, J.D., Hotes, S., 2013. The impact of high tephra loading on late-Holocene carbon accumulation and vegetation succession in peatland communities. Quat. Sci. Rev. 67, 160–175.

Iacovino, et al., 2016. Quantifying gas emissions from the 'Millennium eruption' of Paektu volcano, democratic People's Republic of Korea/China. Sci. Adv. http://dx.doi.org/10.1126/sciadv.1600913.

Jensen, B.J., Pyne-O'Donnell, S., Plunkett, G., Froese, D.G., Hughes, P.D., Sigl, M., McConnell, J.R., Amesbury, M.J., Blackwell, P.G., van den Bogaard, C., Buck, C.E., 2014. Transatlantic distribution of the Alaskan white river ash. Geology 42, 875–878.

Kamite, M., Yamada, K., Saito-Kato, M., Okuno, M., Yasuda, Y., 2010. Microscopic observations of varve sediments from Lake Ni-no-Megata and lake san-no-megata, Oga Peninsula, NE Japan, with reference to the fallout age of the B-Tm tephra. J. Geol. Soc. Jpn. 116, 349–359.

Kang, J.H., et al., 2015. Mineral dust and major ion concentrations in snowpit samples from the NEEM site, Greenland. Atmos. Env. 120, 137–143.

Kim, A., 2011. The historiography of Bohai in Russia. Historian 73, 284–299.

Machida, H., Arai, F., 1983. Extensive ash falls in and around the Sea of Japan from large late Quaternary eruptions. J. Volcanol. Geotherm. Res. 18, 151–164.

Machida, H., Moriwaki, H., Da-Chang, Z., 1990. The Recent Major Eruption of Changbai Volcano and its Environmental Effects, 25. Tokyo Met. Univ., pp. 1–20. Geog. Rep.

Machida, H., Okumura, K., 2007. Recent Large-scale Explosive Eruption of Baegdusan Volcano: Age of Eruption and its Effects on Society. Abstract XVII INQUA Congress 2007, Cairns, Australia.

McLean, D., Albert, P.G., Nakagawa, T., Staff, R.A., Suzuki, T., Smith, V.C., 2016. Identification of the Changbaishan ‘Millennium’(B-Tm) eruption deposit in the Lake Suigetsu (SG06) sedimentary archive, Japan: synchronisation of hemispheric-wide palaeoclimate archives. Quat. Sci. Rev. 150, 301–307.

Miyake, F., Nagaya, K., Masuda, K., Nakamura, T., 2012. A signature of cosmic-ray increase in AD 774-775 from tree rings in Japan. Nature 486, 240–242.

Nakamura, T., et al., 2007. Application of ^{14}C wiggle-matching to support dendrochronological analysis in Japan. Tree-Ring Res. 63, 37–46.

Nanayama, F., Satake, K., Furukawa, R., Shimokawa, K., Atwater, B.F., Shigeno, K., Yamaki, S., 2003. Unusually large earthquakes inferred from tsunami deposits along the Kuril trench. Nature 424, 660–663.

Nemec, M., Wacker, L., Hajdas, I., Gäggeler, H., 2010. Alternative methods for cellulose preparation for AMS measurement. Radiocarbon 52, 1358–1370.

Oppenheimer, C., 2003. Climatic, environmental and human consequences of the largest known historic eruption: Tambora volcano (Indonesia) 1815. Prog. Phys. Geogr. 27 (2), 230–259.

Oppenheimer, C., 2011. Eruptions that Shook the World. Cambridge University Press.

Oppenheimer, C., 2015. Eruption politics. Nat. Geosci. 8 (4), 244–245.

Perlwitz, J., Graf, H.F., 1995. The statistical connection between tropospheric and stratospheric circulation of the Northern Hemisphere in winter. J. Clim. 8 (10), 2281–2295.

Reimer, P.J., Bard, E., Bayliss, A., Beck, J.W., Blackwell, P.G., Bronk Ramsey, C., Buck, C.E., Cheng, H., Edwards, R.L., Friedrich, M., Grootes, P.M., Guilderson, T.P., Haflidason, H., Hajdas, I., Hatté, C., Heaton, T.J., Hoffmann, D.L., Hogg, A.G., Hughen, K.A., Kaiser, K.F., Kromer, B., Manning, S.W., Niu, M., Reimer, R.W., Richards, D.A., Scott, E.M., Southon, J.R., Staff, R.A., Turney, C.S.M., van der Plicht, J., 2013. IntCal13 and Marine13 radiocarbon age calibration curves 0–50,000 years cal BP. Radiocarbon 55 (4), 1869–1887.

Schneider, L., Smerdon, J.E., Büntgen, U., Wilson, R.J.S., Myglan, V.S., Kirdyanov, A.V., Esper, J., 2015. Revising midlatitude summer temperatures back to A.D. 600 based on a wood density network. Geophys. Res. Lett. 42 http://dx.doi.org/10.1002/2015GL063956.

Sigl, M., et al., 2013. A new bipolar ice core record of volcanism from WAIS Divide and NEEM and implications for climate forcing of the last 2000 years. J. Geophys. Res. Atmos. 118, 1151–1169. http://dx.doi.org/10.1029/2012JD018603.

Sigl, M., et al., 2015. Timing and climate forcing of volcanic eruptions for the past 2,500 years. Nature 523, 543–549.

Stoffel, M., et al., 2015. Estimates of volcanic-induced cooling in the Northern Hemisphere over the past 1,500 years. Nat. Geosci. 8, 784–788.

Sun, C., et al., 2014a. Ash from Changbaishan Millennium eruption recorded in Greenland ice: implications for determining the eruption's timing and impact. Geophys. Res. Lett. 41 (2), 694–701.

Sun, C., et al., 2014b. Distribution, geochemistry and age of the Millennium eruptives of Changbaishan volcano, Northeast China – a review. Front. Earth Sci. 8, 216–230.

Synal, H.A., Stocker, M., Suter, M., 2007. MICADAS: a new compact radiocarbon AMS system. Nucl. Instrum. Methods Phys. Res. Sect. B Beam Interact. Mater. Atoms 259, 7–13.

Sun, C., You, H., He, H., Zhang, L., Gao, J., Guo, W., Chen, S., Mao, Q., Liu, Q., Chu, G., Liu, J., 2015. New evidence for the presence of Changbaishan Millennium eruption ash in the Longgang volcanic field, Northeast China. Gondwana Res 28, 52–60.
Wacker, L., et al., 2010a. Micadas: Routine and High-precision Radiocarbon Dating: Radiocarbon, vol. 52, pp. 252–262.
Wacker, L., et al., 2014. Radiocarbon dating to a single year by means of rapid atmospheric C-14 changes. Radiocarbon 56, 573–579.
Wacker, L., Nemec, M., Bourquin, J., 2010b. A revolutionary graphitisation system: fully automated, compact and simple. Nucl. Instr. Methods Phys. Res. B 268 (7–8), 931–934.
Xu, J., et al., 2013. Climatic impact of the Millennium eruption of Changbaishan volcano in China: new insights from high-precision radiocarbon wiggle-match dating. Geophys. Res. Lett. 40, 54–59. http://dx.doi.org/10.1029/2012GL054246.
Yamada, K., Kamite, M., Saito-Kato, M., Okuno, M., Shinozuka, Y., Yasuda, Y., 2010. Late Holocene monsoonal-climate change inferred from Lakes Ni-no-Megata and San-no-Megata, northeastern Japan. Quat. Int. 220 (1–2), 122–132.
Yatsuzuka, S., et al., 2010. ^{14}C wiggle-matching of the B-Tm tephra, Baitoushan volcano, China/North Korea. Radiocarbon 52, 933–940.
Yin, J., Jull, A.J.T., Burr, G., Zheng, Y., 2012. A wiggle-match age for the Millennium eruption of Tianchi volcano at Changbaishan, northeastern China. Quat. Sci. Rev. 47, 150–159. http://dx.doi.org/10.1016/j.quascirev.2012.05.015.
Zielinski, G.A., 1995. Stratospheric loading and optical depth estimates of explosive volcanism over the last 2100 years derived from the Greenland Ice Sheet Project 2 ice core. J. Geophys. Res. 100 (D10), 20937–20955. http://dx.doi.org/10.1029/95JD01751.